Onsager Model for the Structure of Rigid Rods Confined on a Spherical Surface

Wu-Yang Zhang, Ying Jiang, and Jeff Z. Y. Chen*

Guelph-Waterloo Physics Institute and Department of Physics and Astronomy, University of Waterloo, Ontario, Canada, N2L 3G1

(Received 23 August 2011; published 30 January 2012)

Recent studies have suggested that a monolayer of self-avoiding hard rods confined on a spherical surface may display a distribution texture corresponding to splay, tennis-ball, rectangle, or cut-and-rotate splay symmetries. We investigate the system on the basis of a generalized Onsager model which includes both excluded-volume and entropic effects. The numerical solution indicates that the splay state, where on average rods line up in parallel to the longitudinal lines on the spherical surface, is the only stable state.

DOI: 10.1103/PhysRevLett.108.057801 PACS numbers: 61.30.Cz, 61.30.Hn, 64.70.M−, 82.70.Dd

Introduction.—Consider a two-dimensional liquid confined on a spherical surface of radius R, consisting of N volume-excluding, rodlike particles of length L. At low relative surface coverage density, $NL^2/4\pi R^2$, to maximize the orientational and positional entropies, no particular pattern would form by these rods. Beyond a transition density, coupled orientational and positional ordering starts to emerge, giving rise to a configurational texture on the spherical surface.

This model belongs to a class of recently studied systems that points to the possibility of producing a multivalent spherical colloid particle by coating a micron-size sphere with a layer of anisotropic particles [1], dispersing a hard sphere in a nematic solution [2], or creating emulsion droplets with nematic liquids [3,4]. Such structures break the azimuthal symmetry of a splay distribution on a spherical surface, shown in Fig. 1(a). Practical applications using these structures in designing new smart materials have been explored [4–6]. Of particular interest is the tetrahedral structure, which contains four $+1/2$ defects appearing at the vertices of a tetrahedron on the spherical surface, shown in Fig. 1(b), two on the xz plane near the north pole and two on the yz plane near the south pole. Theoretical studies based on the Frank elastic energy [1,7,8], Landau–de Gennes free energy [2,9], and lattice nematic shell Lebwohl-Lasher model [10,11] of related systems predicted such a structure.

Could a tetrahedral configuration exist in the current model of volume-excluding rigid rods on a spherical surface? Or, even loosely, instead of having four defects located exactly at the corners of an equal-sided tetrahedron, can a tennis-ball state exist where the vector joining the two defects near the north pole is perpendicular to the vector joining the other pair near the south pole [Fig. 1(b)]? Recent Monte Carlo simulations of *thin* rigid rods confined on a spherical surface ruled out the existence of the perfect tetrahedral tennis-ball structure [12,13]. Instead, other possible defect structures have been suggested. On the basis of a Monte Carlo snapshot, Bates [13] showed a configuration that resembles a tennis-ball texture but is more similar to splay; in another simulation snapshot the vector joining the two defects near the north pole is parallel to the vector joining the other pair near the south pole, four defects forming corners of a rectangle on the xz plane shown in Fig. 1(c). Shin *et al.* [12] and Bates [13] also suggested the existence of a so-called "cut-and-rotate" splay structure—the pattern resembles cutting a perfect splay state along the north-south pole plan and then rotating one of the hemispheres by an angle about the y axis, shown in Fig. 1(d).

Model.—In this Letter, we consider numerical solutions of a free-energy model, generalizing the Onsager interaction between rodlike particles in a flat space to a system of N rigid "rods" occupying the surface of a sphere of radius R. These rods are not exactly straight, each being a geodesic segment of length L with no thickness, on the spherical surface along a great circle. A density distribution function can be used to characterize the system, $\varrho(\mathbf{r}, \mathbf{u})$, where $\mathbf{r}$ and $\mathbf{u}$ are the position vector and tangent unit vector, respectively, of the center of mass of a rod, $\int \varrho(\mathbf{r}, \mathbf{u}) d\mathbf{u} d\mathbf{r} = N$. Following the well-known Onsager approach, which includes a second-virial term, we can write down the free energy of the system [14],

$$\beta F = \int \varrho(\mathbf{r}, \mathbf{u}) \ln[8\pi^2 R^2 \varrho(\mathbf{r}, \mathbf{u})] d\mathbf{r} d\mathbf{u} + \frac{1}{2} \int \varrho(\mathbf{r}, \mathbf{u}) w(\mathbf{r}, \mathbf{u}; \mathbf{r}', \mathbf{u}') \varrho(\mathbf{r}', \mathbf{u}') d\mathbf{r} d\mathbf{u} d\mathbf{r}' d\mathbf{u}'. \quad (1)$$

The second term contains a function $w(\mathbf{r}, \mathbf{u}; \mathbf{r}', \mathbf{u}')$ that depends on variables $(\mathbf{r}, \mathbf{u})$ and $(\mathbf{r}', \mathbf{u}')$, representing the coordinates of the centers of mass of two rods; this function

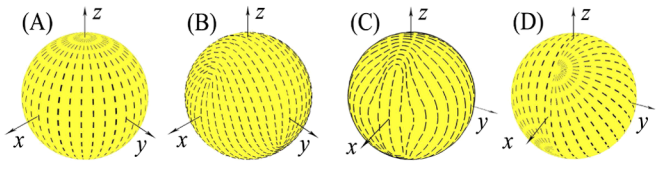

FIG. 1 (color online). Idealized illustration of four possible structures considered in this work: splay (a), tennis ball (b), rectangle (c), and cut-and-rotate splay (d).

takes value 1 if any parts of the two rods overlap and 0 otherwise. Apart from a trivial linear term in $\varrho(\mathbf{r}, \mathbf{u})$ introduced for later convenience, the first term arises because of both orientational and translational entropies. The free energy as a functional of $\varrho(\mathbf{r}, \mathbf{u})$ needs to be minimized; the result is the stable-state distribution function for the system.

In order to minimize the free energy, we expanded $\varrho(\mathbf{r}, \mathbf{u})$ in terms of spherical harmonics Y_{lm} and Fourier bases U_n,

$$\varrho(\mathbf{r}, \mathbf{u}) = \frac{N}{R^2} \sum_{lmn} \phi_{lmn} Y_{lm}(\Theta, \Phi) U_n(\theta), \tag{2}$$

where $\mathbf{r}$ is represented by the spherical coordinates Θ and Φ and $\mathbf{u}$ by the angle θ that $\mathbf{u}$ makes with respect to a longitudinal line. Except for the leading term that renders the normalization condition, all other expansion coefficients ϕ_{lmn} were adjusted to minimize the free energy. We aim at finding an exact solution of the free-energy model using a multiple-variable approach, so that the free energy can be minimized with no ambiguous approximations. We truncated the expansion beyond $l = 8$ and $n = 8$ terms and estimated that the truncation error does not exceed the size of symbols in the following illustrations. The detailed numerical approach, together with a computational procedure to deal with both terms in (1), will be documented elsewhere.

Free-energy minimum.—This model has a trivial solution corresponding to an isotropic state, $\varrho_{\text{iso}}(\mathbf{r}, \mathbf{u}) = N/8\pi^2 R^2$. The free energy of the system can be written,

$$\beta F_{\text{iso}} = N \ln N + \frac{N^2 L^2}{4\pi^2 R^2} \operatorname{sinc} \frac{L}{2R}, \tag{3}$$

where $\operatorname{sinc}(x) = \sin(x)/x$. We then consider the free-energy difference per rod,

$$\tilde{f} \equiv (\beta F - \beta F_{\text{iso}})/N. \tag{4}$$

An examination of $\tilde{f}$ shows that out of three variables, L, R, and N, only two reduced parameters are important, L/R, and the reduced surface density,

$$\rho L^2 = N L^2/(4\pi R^2). \tag{5}$$

All three solid curves in Figs. 2(a)–2(c) represent the same ground-state splay energy $\tilde{f}$ obtained from the numerical minimization for $L/R = 0.5$. The number of surviving terms in the expansion (2) varies according to the underlying symmetries of a particular structure in Fig. 1. Because the splay conformation has a higher symmetry than the other three, all terms corresponding to the splay conformation ("splay terms") exist in the expansions of the other three free energies. We employed four different processes of conducting the minimization search. Each process corresponds to a study of a particular type of conformation; we directly searched for the free-energy minimum, varying the undetermined coefficients of all relevant terms and removing all other terms that violate the symmetry properties of such a conformation. By the end of the search, all four processes converge to one single result: only the coefficients of the splay terms are significantly present and coefficients of the nonsplay terms vanish. Within the range of parameter space studied, $L/R = [0.1, 1]$, in high ρL^2 we found that the splay conformation is the only stable ground state of the free energy in (4).

In order to dissect the structures associated with the nonsplay conformations, we took another approach in our numerical study. Each nonsplay conformation is characterized by a leading term in the free-energy expansion, tennis ball by the $(l, m, n) = (3, 2, 0)$ term, rectangle by the $(2, 2, 0)$ term, and cut-and-rotate splay by the $(3, -2, 0)$ term. These are the terms that do not exist in a splay state. We *fixed* the coefficients of these terms (hence, enforced symmetry breaking into a particular structure) in small increments and numerically searched for the free-energy minima by varying other coefficients. Examples of such

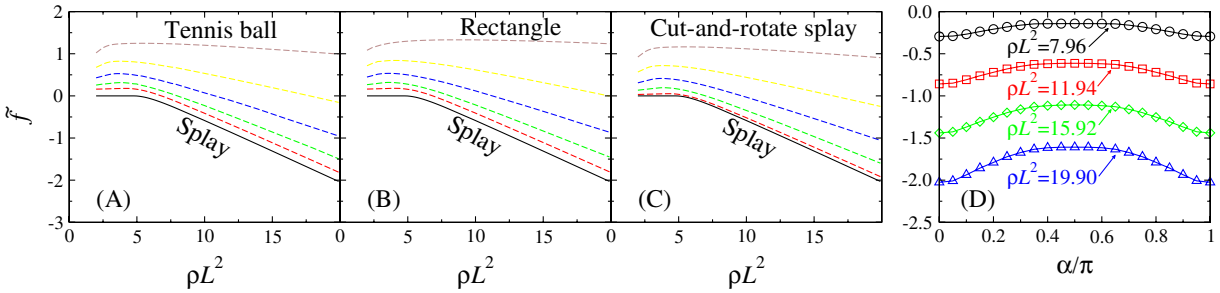

FIG. 2 (color online). Minimized Onsager free-energy difference, Eq. (4), plotted as a function of reduced number density ρL^2 [(a)–(c)] and as a function of the cut-and-rotate angle α, for $L/R = 0.5$. The solid curve (black) in (a)–(c) is the splay branch of the free energy. Dashed lines were produced by fixing the leading symmetry-breaking term in the density distribution expansion (2): $\phi_{3,2,0}$ fixed at -0.1 (brown), -0.08 (yellow), -0.06 (blue), -0.04 (green), and -0.02 (red) from the top to bottom curves for tennis ball (a), $\phi_{2,2,0}$ at 0.1 (brown), 0.08 (yellow), 0.06 (blue), 0.04 (green), and 0.02 (red) for rectangle (b), and $\phi_{3,-2,0}$ at 0.1 (brown), 0.08 (yellow), 0.06 (blue), 0.04 (green), and 0.02 (red) for cut-and-rotate splay (c). In (d), circles, squares, diamonds, and triangles represent $\rho L^2 = 7.96$, 11.94, 15.92, and 19.90, respectively.

minimizations are displayed in Figs. 2(a)–2(c) for $L/R = 0.5$. Plots for other values of L/R in the range $[0.1, 1]$ share the same features, except for shifts in $\tilde{f}$ magnitude and splay bifurcation point. All calculations demonstrate that other possible conformations have a $\tilde{f}$ above the splay ground state.

The consideration of the existence of a ground-state tennis-ball conformation stemmed from an analysis of elastic theory of the orientational field generated by the particles. In a one-Frank-constant approximation in two dimensions [1,7], K_2 is absent and $K_1 = K_3$, where K_1 for splay distortion, K_2 for twist distortion, and K_3 for bend distortion are the Frank constants; the Frank energy can be mapped into the energy of the two-dimensional ferromagnetic XY model [15]. Then one can show that the free energy is proportional to the square of the defect index. The tennis-ball conformation contains four $+1/2$ defects (the orientational field turns a π angle around each defect) and the splay conformation contains two $+1$ defects (the orientational field turns 2π around each defect). Thus, within this assumption, the tennis-ball conformation has a lower energy than that of the splay [1,7].

Here we deal with the specific system of thin rods. We can introduce a trial function describing the angular distribution about a vector director field $\vec{n}(\mathbf{r})$. An expansion of the Onsager free energy, Eq. (1), in terms of the first spatial derivatives, exactly recovers the structure of the Frank energy. According to Refs. [16,17], such a treatment yields an estimate $K_1 \ll K_3$, which does not satisfy the one-Frank-constant approximation to start with. Hence, it is not surprising that the tennis-ball configuration is not the ground state in the current model [12,13].

Confined systems consisting of molecules with some semiflexibility might display the tennis-ball texture in high density. An interesting real system is the liquid of 5CB molecules [4], which has $K_1 \approx K_3$ [18], consistent with the one-Frank-constant condition; experimentally, nonsplay textures were observed [4]. Another related system, though theoretical, is a long self-avoiding semiflexible polymer chain confined on a spherical surface. Because of the flexibility along the chain, K_3 now becomes comparable to K_1. Using Monte Carlo simulations, we recently concluded that this system displays a disorder-order transition, where the ordered state always accompanies the tennis-ball symmetry [19].

Using Monte Carlo simulations on a spherical surface, Shin *et al.* found the simulation evidence of the so-called cut-and-rotate splay conformation in closely packed *straight* hard rods [12], where $L/R \approx 0.4$ and $\rho L^2 \approx 14$. In an idealized picture [Fig. 1(d)] where the director field *perfectly* aligns along the longitudinal lines, the cut-and-rotate splay configuration has a similar Frank energy as the splay state, according to the analysis in Ref. [12]. However, the angular distribution about the director field of this conformation contains a sharp change at the cutting circle. Following the trial function approach and taking a complete expansion of the Onsager free energy in terms of spatial derivatives of $\vec{n}(\mathbf{r})$, we can show that only the quadratic derivative terms correspond to the Frank energy [16]. Higher order derivatives, hence the unexpanded version of the Onsager free energy, disfavor such sharp changes by raising the free energy of the system. This effect rules out the cut-and-rotate splay in the current system. It should be noted that our model deals with geodesic rods, which are not exactly straight rods simulated in Refs. [12,13]; despite this, we still expect the same qualitative physical picture in the small L/R limit.

To show the cut-and-rotate effects, we took the density distribution $\varrho_{\mathrm{spl}}(\mathbf{r}, \mathbf{u})$ from the minimized splay state, cut it through the xz plane, and rotated the distributions along the positive and negative y axes by a relative α angle. In Fig. 2(d), we display the cut-and-rotate $\tilde{f}$ as a function of the rotation angle α for $L/R = 0.5$. From the plot, we can see that the cut-and-rotate splay structure has a higher free energy in comparison with that of the splay state ($\alpha = 0$ or π). Systems of other L/R values have similar features. This analysis, together with the symmetry-based analysis in Figs. 2(a)–2(c), precludes the probability that cut-and-rotate splay is a stable state within the validity of the free-energy model in (1).

Isotropic-splay transition.—Here we examine two order parameters that characterize the overall ordering of the isotropic-splay transition of the system. One of which, Ω, concerns the global orientational order,

$$\Omega = N^{-1} \int \cos 2\theta \varrho(\mathbf{r}, \mathbf{u}) d\mathbf{u} d\mathbf{r} = 2\pi\phi_{002}. \quad (6)$$

The other parameter, Σ, describes the global spatial order,

$$\Sigma = N^{-1} \int P_2(\cos\Theta) \varrho(\mathbf{r}, \mathbf{u}) d\mathbf{u} d\mathbf{r} = \sqrt{8/5}\pi\phi_{200}. \quad (7)$$

A positive Ω in the anisotropic region implies that the rods tend to line up in the parallel direction to the longitudinal lines; a negative Σ in the anisotropic region means that the

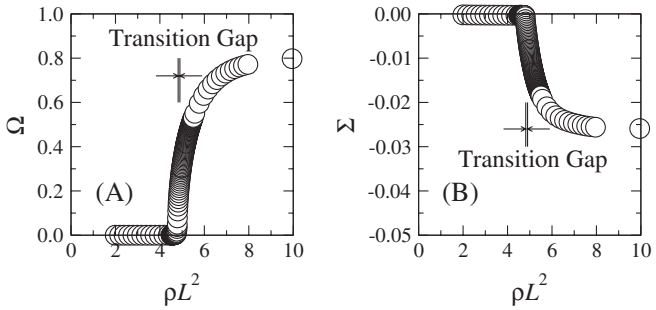

FIG. 3. Orientational and positional order parameters, (a) Ω and (b) Σ, plotted as functions of reduced density, ρL^2, for $L/R = 0.5$. Data points associated with nonzero Ω and Σ were produced from splay configurations. The area inside the two vertical lines indicates a narrow transition region.

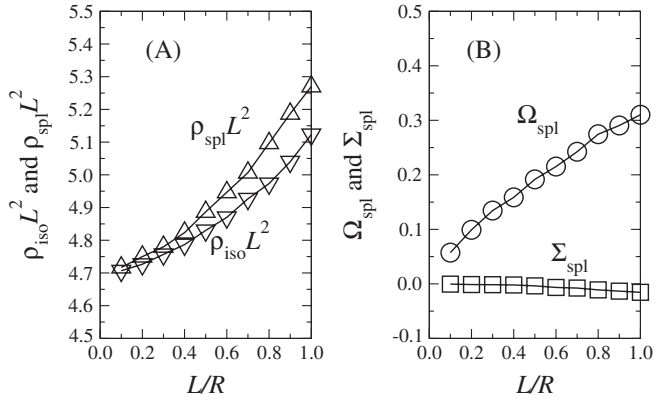

FIG. 4. (a) Transition densities $\rho_{iso}L^2$ (down triangles) and $\rho_{spl}L^2$ (up triangles), and (b) orientational and spatial order parameters, Ω and Σ, at $\rho_{spl}L^2$ plotted as functions of L/R.

density distribution has a peak in the equator region of the spherical surface.

The order-parameter plots in Fig. 3 follow the splay solution of the model and give us the approximate location of the transition density for the disorder-splay phase transition (a bifurcation point). We can substitute (2) into (4) to produce a Landau expansion of $\tilde{f}$ in terms of ϕ_{lmn}. A close examination of the expansion, however, reveals the existence of cubic terms, which couple positional order with orientational order, in systems where $L/R \neq 0$.

Following a free-energy analysis identical to the one used in studying the first-order isotropic-nematic transition of a lyotropic system of rods [20], we can determine the transition densities $\rho_{iso}L^2$ and $\rho_{spl}L^2$ by equating the osmotic pressures and chemical potentials. These densities are plotted in Fig. 4(a) by down and up triangles, respectively, for the range $L/R = [0.1, 1]$ studied in this work. The first-order transition gap $\rho_{iso} - \rho_{spl}$ becomes wider in larger L/R systems and converges to zero in the limit of a flat two-dimensional system ($L/R \to 0$). This fact implies that the first-order disorder-splay transition reduces to a continuous isotropic-nematic transition as $L/R \to 0$, within the validity of the Onsager model; the numerical asymptotic reduced transition density at $L/R = 0$, $\rho_c L^2$ (numerical) $= 4.71$, is consistent with the analytical value found earlier $\rho_c L^2$ (theoretical) $= 3\pi/2$ [21,22]. The first-order nature of the disorder-splay transition in finite L/R systems can be compared to the first-order nature of the isotropic-nematic transition in a three-dimensional system [20,23].

In a typical plot given in Fig. 3 where ρ continually changes, we can divide ρ into three regions. In the $\rho \leq \rho_{iso}$ or $\rho \geq \rho_{spl}$ region, the system is either in a disorder or splay state. In the $\rho_{iso} < \rho < \rho_{spl}$ region, the system is in a mixed disorder-splay state with a possible interface. For comparison, in a lyotropic liquid crystal system, an isotropic-nematic interface can be stabilized when the overall number density is between the two transition densities [24–27].

As it turns out, in a Monte Carlo simulation where the critical fluctuations existed, Frenkel and Eppenga [28] showed that the two-dimensional isotropic-nematic transition in a flat space is a Kosterlitz-Thouless (KT) transition. The model in the current work is of a mean-field nature and does not capture coherent critical fluctuations. The relationship between the first-order disorder-splay transition of rods on a spherical surface and the KT isotropic-nematic transition of rods in a flat surface remains to be explored.

Summary.—We examined a free-energy model on the basis of a generalized Onsager approximation for rigid rods confined on the spherical surface and interacting with each other through the excluded-volume interaction. The model does not contain phenomenological parameters and properly includes major entropic contributions. We developed a numerical method which allows us to minimize the free energy, adjusting the density distribution function. We found that the free-energy minimum corresponds to a stable splay state and that the tennis-ball, rectangle, and cut-and-rotate splay configurations are all not stable, within a significantly wide parameter region searched computationally. The properties of the disorder-splay transition were also discussed.

The authors wish to thank NSERC for financial support and SHARCNET for providing computational time.

*jeffchen@uwaterloo.ca

[1] D. R. Nelson, Nano Lett. **2**, 1125 (2002).
[2] M. Huber and H. Stark, Europhys. Lett. **69**, 135 (2005).
[3] A. Fernández-Nieves, V. Vitelli, A. S. Utada, D. R. Link, M. Márquez, D. R. Nelson, and D. A. Weitz, Phys. Rev. Lett. **99**, 157801 (2007).
[4] T. Lopez-Leon, V. Koning, K. B. S. Davaiah, V. Vitelli, and A. Fernandez-Nieves, Nature Phys. **7**, 391 (2011).
[5] K. M. Ho, C. T. Chan, and C. M. Soukoulis, Phys. Rev. Lett. **65**, 3152 (1990).
[6] F. Li, W. C. Yoo, M. B. Beernink, and A. Stein, J. Am. Chem. Soc. **131**, 18 548 (2009).
[7] T. C. Lubensky and J. Prost, J. Phys. II (France) **2**, 371 (1992).
[8] V. Vitelli and D. R. Nelson, Phys. Rev. E **74**, 021711 (2006).
[9] S. Kralj, R. Rosso, and E. G. Virga, Soft Matter **7**, 670 (2011).
[10] G. Skačej and C. Zannoni, Phys. Rev. Lett. **100**, 197802 (2008).
[11] M. A. Bates, G. Skačej, and C. Zannoni, Soft Matter **6**, 655 (2010).
[12] H. Shin, M. J. Bowick, and X. Xing, Phys. Rev. Lett. **101**, 037802 (2008).
[13] M. A. Bates, J. Chem. Phys. **128**, 104707 (2008).
[14] L. Onsager, Ann. N.Y. Acad. Sci. **51**, 627 (1949).

[15] D. R. Nelson and R. A. Pelcovits, Phys. Rev. B **16**, 2191 (1977).
[16] J. P. Straley, Phys. Rev. A **8**, 2181 (1973).
[17] A. Poniewierski and R. Hołyst, Phys. Rev. A **41**, 6871 (1990).
[18] J. D. Bunning, T. E. Faber, and P. L. Sherrell, J. Phys. (Paris) **42**, 1175 (1981).
[19] W.-Y. Zhang and J. Z. Y. Chen, Europhys. Lett. **94**, 43 001 (2011).
[20] T. Odijk, Macromolecules **19**, 2313 (1986).
[21] R. F. Kayser and H. J. Raveché, Phys. Rev. A **17**, 2067 (1978).
[22] Z. Y. Chen, Phys. Rev. Lett. **71**, 93 (1993).
[23] A. R. Khokhlov and A. N. Semenov, Physica (Amsterdam) **108A**, 546 (1981).
[24] Z. Y. Chen and J. Noolandi, Phys. Rev. A **45**, 2389 (1992).
[25] Z. Y. Chen, Phys. Rev. E **47**, 3765 (1993).
[26] S.-M. Cui, O. Akcakir, and Z. Y. Chen, Phys. Rev. E **51**, 4548 (1995).
[27] Y. Jiang and J. Z. Y. Chen, Macromolecules **43**, 10 668 (2010).
[28] D. Frenkel and R. Eppenga, Phys. Rev. A **31**, 1776 (1985).